CHEMISTRY
A EUROPEAN JOURNAL

FULL PAPER

DOI: 10.1002/chem.201201299

Hydrogen-Bonding-Mediated Vesicular Assembly of Functionalized Naphthalene–Diimide-Based Bolaamphiphile and Guest-Induced Gelation in Water

Mijanur Rahaman Molla and Suhrit Ghosh*[a]

Abstract: This paper describes the spontaneous vesicular assembly of a naphthalene–diimide (NDI)-based non-ionic bolaamphiphile in aqueous medium by using the synergistic effects of π-stacking and hydrogen bonding. Site isolation of the hydrogen-bonding functionality (hydrazide), a strategy that has been adopted so elegantly in nature, has been executed in this system to protect these moieties from the bulk water so that the distinct role of hydrogen bonding in the self-assembly of hydrazide-functionalized NDI building blocks could be realized, even in aqueous solution. Furthermore, the electron-deficient NDI-based bolaamphiphile could engage in donor–acceptor (D–A) charge-transfer (CT) interactions with a water-insoluble electron-rich pyrene donor by virtue of intercalation of the latter chromophore in between two NDI building blocks. Remarkably, even when pyrene was located between two NDI blocks, intermolecular hydrogen-bonding networks between the NDI-linked hydrazide groups could be retained. However, time-dependent AFM studies revealed that the radius of curvature of the alternately stacked D–A assembly increased significantly, thereby leading to intervesicular fusion, which eventually resulted in rupturing of the membrane to form 1D fibers. Such 2D-to-1D morphological transition produced CT-mediated hydrogels at relatively higher concentrations. Instead of pyrene, when a water-soluble carboxylate-functionalized pyrene derivative was used as the intercalator, non-covalent tunable in-situ surface-functionalization could be achieved, as evidenced by the zeta-potential measurements.

Keywords: gels · hydrogen bonds · surface chemistry · vesicles · water

Introduction

The self-assembly of amphiphilic molecules and macromolecules has emerged as an exciting field of research in interdisciplinary fields that range from biology to materials science. Various classical small-molecule amphiphiles[1] (single-tail surfactants, gemini surfactants, bolaamphiphiles, phospholipids, etc.) and amphiphilic polymers[2] have produced elegant nanoscale assemblies, such as spherical and rod-like micelles, vesicles, fractals, fibers, nanotubes, etc. Amazingly, most of these amphiphilic molecules, be they small molecules or macromolecules, are structurally identical in a broad sense, that is, they consist of hydrophobic and hydrophilic segments, which differ in terms of their relative length, volume, and how they are covalently linked to each other. Over the last two decades, chemists have developed enormous knowledge to generate a diverse range of supramolecular materials,[3] mostly in organic medium, by virtue of utilizing various directional non-covalent forces, such as π-stacking, hydrogen bonding, charge-transfer (CT) interactions, and metal–ligand coordination. In an attempt to realize the implications of such directional interactions in aqueous medium, amphiphiles that contain π-conjugated chromophores,[4] as well as those that can be generated by using non-covalent forces (commonly known as supramolecular amphiphiles[5]), have been investigated with great interest in the recent past. An additional motivation to study this subclass of amphiphiles stems from the possibility of relating their rich photophysical properties[6] to biological applications, such as biosensing, imaging, etc. Most of the reported π-conjugated amphiphiles only differ from classical amphiphiles in terms of replacing the hydrophobic segment with a chromophore moiety. A natural next step towards enriching the structural diversity of amphiphiles in general would be to make multiple directional force work effectively in tandem. In this context, the obvious choice would be hydrogen-bonding interactions,[7a] considering the diverse range of hydrogen-bonding synthons[7b] that are available today in the chemist's toolbox. This choice is also inspired by the amazing programmed assembled structures (such as folded proteins and the DNA double-helix) that are fabricated in nature. However, examples of the hydrogen-bonding-directed self-assembly of abiotic building blocks in aqueous medium are still rare,[8] presumably because of the inherent difficulty that is associated with competitive hydrogen-bonding interactions with the solvent molecules. Thus, biomimicking in the context of self-assembly (in terms of structure and not even function) is still mostly confined to the domain

[a] M. R. Molla, Dr. S. Ghosh
Polymer Science Unit
Indian Association for the Cultivation of Science
2A & 2B Raja S. C. Mullick Road
Kolkata, INDIA-7000 32
E-mail: psusg2@iacs.res.in

Supporting information for this article is available on the WWW under http://dx.doi.org/10.1002/chem.201201299.

© 2012 Wiley-VCH Verlag GmbH & Co. KGaA, Weinheim
WILEY ONLINE LIBRARY
These are not the final page numbers!

of non-polar organic media. 1,4,5,8-Naphthalene–tetracarboxylic-acid–diimide (NDI)-derivatives[9] have been extensively explored as a building block for the generation of various supramolecularly assembled systems, both in organic- and aqueous media, owing to their n-type semiconductivity,[10] propensity for π-stacking, and electron-accepting nature. Examples of such systems include organogels,[11] catenanes,[12] rotaxanes,[13] foldamers,[14] nanotubes,[4b] hydrogels,[15] nanoparticles,[4c] supramolecular photosystems,[16] and synthetic ion-channels.[17]

In the recent past, we have also used NDI-based systems to demonstrate self-sorting[18] and to understand structure-property relationships[19] in organogels. Herein, we report the spontaneous vesicular assembly of **NDI-1** (Scheme 1) in aqueous medium and CT-interaction-mediated 2D-to-1D vesicle-to-hydrogel[20–21] transformations in the presence of an electron-rich pyrene intercalator. In **NDI-1**, the peripheral hydrophilic wedge is attached to the NDI core by a hydrazide group, which has been demonstrated[19a] to be a very effective strategy for hydrogen-bonding-mediated self-assembly in non-polar organic media. We envisioned that such site isolation of the hydrazide groups from bulk water is essential for these groups to be involved in hydrogen-bonding interactions among themselves and, thus, by design, they are rigidly linked between two hydrophobic aromatic segments.

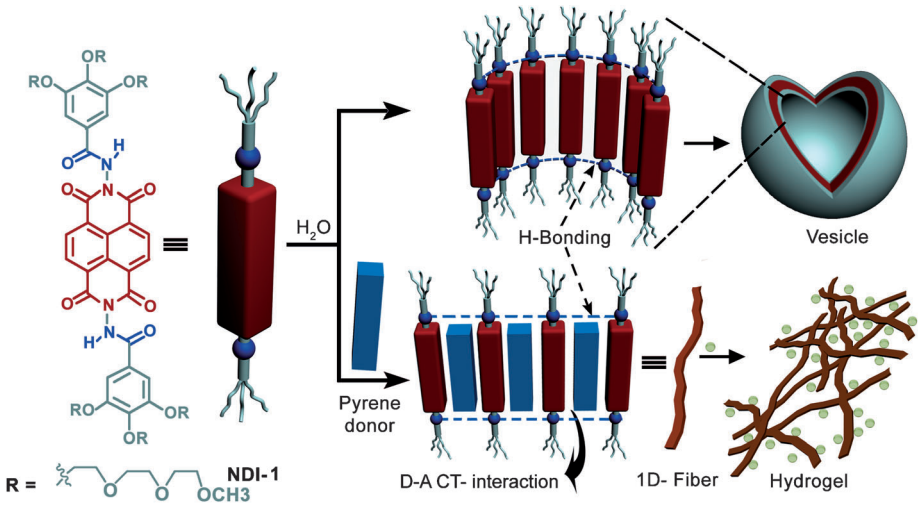

Scheme 1. Top) Structure and vesicular assembly of **NDI-1**. Bottom) CT-interaction-mediated morphological transition (2D-to-1D vesicle-to-fiber) and gelation by pyrene intercalation.

Results and Discussion

Self-assembly: In THF, which is a good solvent for NDI, sharp absorption bands in the range 300–400 nm were noted (Figure 1 a) with vibronic features, which indicated the existence of the free monomer. Going from THF to water, a decrease in the band intensity was observed with a concomitant red shift of about 5 nm, in addition to the intensity reversal of the first (375 nm) and second vibronic peaks[22] (356 nm), thus suggesting the presence of π-stacking. Concentration-dependent UV/Vis studies (Figure 1 b) revealed that, at lower concentrations, the spectroscopic features in water resembled those in THF, thus suggesting disassembly. The critical aggregation concentration of **NDI-1** was estimated to be 0.35 mM from the concentration dependence of the extinction coefficient (ε) at 375 nm (see the Supporting Information, Figure S1).

To probe the role, if any, of hydrogen-bonding in the assembly process, the FTIR spectra of **NDI-1** in THF and water were compared. The peak that corresponded to the

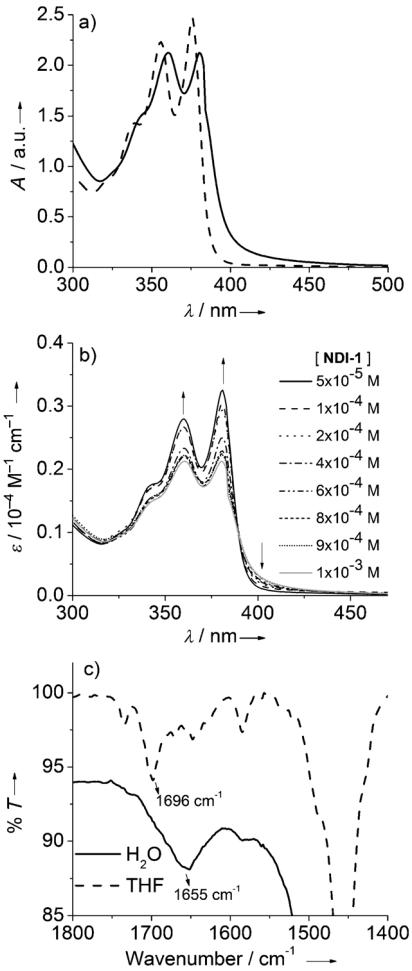

Figure 1. a) UV/Vis spectra of **NDI-1** (1 mM) in THF (dotted line) and water (solid line). b) Concentration-dependent UV/Vis spectra of **NDI-1** in water; arrows indicated spectroscopic changes with dilution. c) FTIR spectra (selected region) of **NDI-1** (2 mM) in THF (dotted line) and water (solid line).

© 2012 Wiley-VCH Verlag GmbH & Co. KGaA, Weinheim

These are not the final page numbers!

carbonyl stretch of the hydrazide group shifted from 1696 cm^{-1} in THF to 1655 cm^{-1} in water, thereby suggesting the involvement of hydrazide groups in hydrogen-bonding (Figure 1c). To ascertain that such hydrogen-bonding exists, particularly between the hydrazide groups and not with the bulk water, the spectroscopic behavior of two control molecules (**1** and **NDI-2**, Figure 2a) were compared with that of **NDI-1**.

Compound **1**, which is a water-soluble intermediate in the synthesis of **NDI-1**, contains a bare hydrazide group and does not contain a NDI chromophore, whilst **NDI-2** is structurally more similar to **NDI-1**, except that the amide functionality is linked to the NDI core by a relatively flexible ethylene linker. In the FTIR spectra of compound **1**, the peak that was due to the hydrazide carbonyl group appeared at almost the same position (Figure 2b) in THF (1647 cm^{-1}) and water (1643 cm^{-1}), which shows that the observed solvent-dependent (THF and water) spectroscopic shift of about 40 cm^{-1} for the same functional group in **NDI-1** (Figure 1c) was indeed due to hydrogen bonding between the hydrazide groups and not with the bulk water. Interestingly, even for **NDI-2**, the IR spectrum revealed very similar positions of the peaks that corresponded to the carbonyl stretching of the amide group in THF and water (Figure 2c). This result provides strong evidence in support of the necessity of the rigid placement of the hydrazide groups in **NDI-1** for the desired hydrogen-bonding-mediated self-assembly. Furthermore, in the UV/Vis spectra of **NDI-2**, a broad charge-transfer band was noticed, even in THF, which was more intense in water (see the Supporting Information, Figure S2).

This band is possibly due to folding-induced donor-acceptor-donor-type interactions[14] between the electron-rich trialkoxybenzamide ring and the NDI acceptor, which could happen owing to the flexible spacer and the lack of hydrogen-bonding between the amide groups. In biological systems, denaturing of the protein is achieved in the presence of excess urea, which is believed to interrupt the hydrogen-bonding between the amide groups.[23] To test whether such a possibility exists in this abiotic system, urea was added to a solution of **NDI-1** (1 mM) and, in the presence of 1.8 M urea, the aggregated spectrum of **NDI-1** completely reverted back to the monomeric spectra (Figure 2d), thus reconfirming the involvement of hydrogen-bonding in the assembly process. Notably, in the case of protein denaturation, it is commonly accepted[23] that, initially, urea is adsorbed onto the hydrophilic surface of a globular protein before its penetrates into the hydrogen-bonding site. Similarly, it is conceivable that, in our system, urea might have been initially adsorbed onto the peripheral hydrophilic oligo-oxyethylene segments, which helped them to diffuse further inside, in the vicinity of the hydrazide groups and compete with the intermolecular hydrogen-bonding network.

Vesicular assembly: AFM images of self-assembled **NDI-1** (Figure 3a and the Supporting Information, S3) showed the presence of spherical aggregates with heights and widths in the range (3.5 ± 0.2) nm and 50–70 nm, respectively. TEM images (Figure 3b) also revealed similar spherical objects (diameter ≈ 50–80 nm) with thin walls and hollow interiors, thus suggesting a vesicular morphology of **NDI-1**. The size of the aggregates was determined to be (50 ± 10) nm by DLS measurement (see the Supporting Information, Figure S4), which corroborates well with the microscopic results. We proposed that the **NDI-1** bolaamphiphile initially formed an elongated 1D assembly through π-stacking interactions between the NDI chromophores and hydrogen-bonding between the hydrazide functionalities, which then formed a closed monolayer membrane. The curvature that was required for membrane formation (Scheme 1) might have been generated from minimize exposure of the termi-

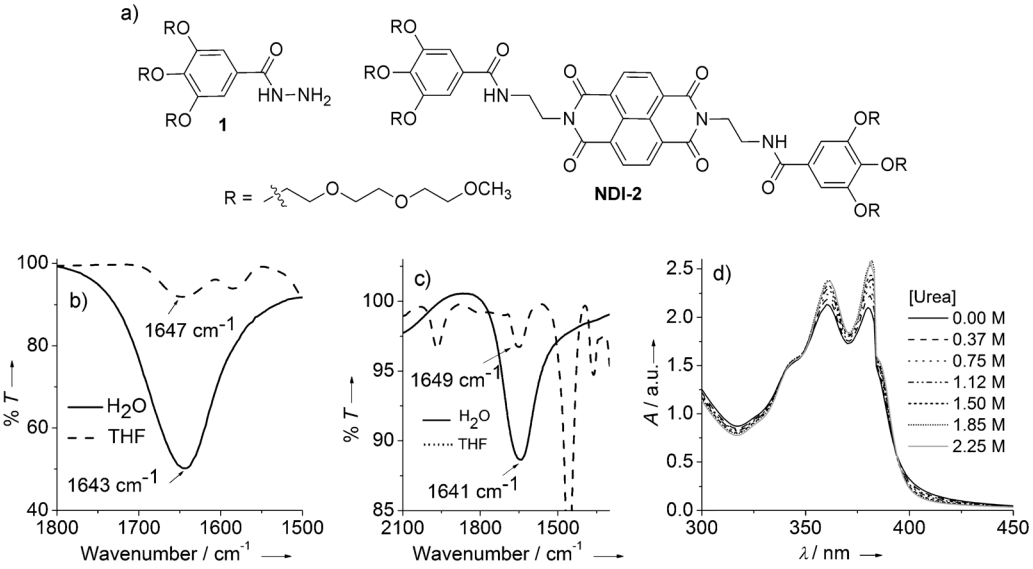

Figure 2. a) Structures of the control molecules. Solvent dependent FTIR spectra of compound **1** (b) and **NDI-2** (c); $c = 2$ mM. d) Effect of urea addition on the UV/Vis spectra of an aqueous solution of **NDI-1** (1 mM).

© 2012 Wiley-VCH Verlag GmbH & Co. KGaA, Weinheim

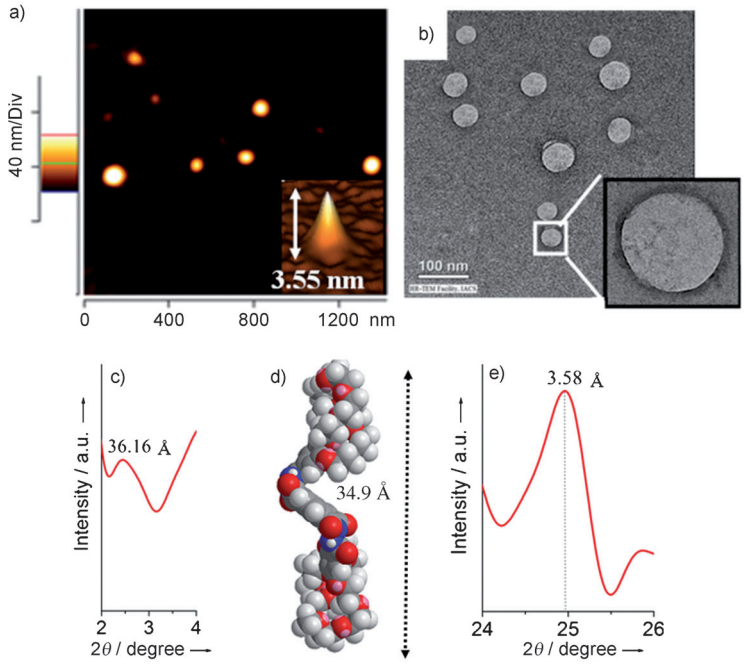

Figure 3. a) AFM height image (inset shows 3D view of one vesicle) and b) TEM image of **NDI-1** vesicles; c,e) selected regions of the XRD pattern of **NDI-1**, and the energy-minimized structure (d).

nal hydrophobic NDI surface to water. The proposed formation of the membrane monolayer could be substantiated by powder XRD pattern of **NDI-1**, wherein sharp reflection was noted (Figure 3c) in the low-angle region ($d=36.16$ Å), which closely matched with the theoretically calculated fully extended length of one **NDI-1**molecule (34.90 Å, Figure 3d). Furthermore, a peak was also noticed at $d=3.58$ Å (Figure 3e), thus reconfirming π-stacking between the NDI chromophores in the organized membrane.

To test its properties as a container, an aqueous solution of **NDI-1** was treated with a hydrophobic dye, Nile red, which has negligible solubility in water on its own. The emission spectra of Nile red was monitored for a series of solutions at a fixed dye concentration with various amount of **NDI-1**. Beyond a certain concentration of **NDI-1**, a strong emission from the dye was noticed, thus suggesting encapsulation (Figure 4a). The emission intensity at 606 nm was monitored as a function of the concentration of **NDI-1** and, from the inflection point of the plot (Figure 4b), the CAC was estimated to be 0.28 mM, which closely matched with the concentration-dependent UV/Vis studies (Figure 1b). Red-light-emitting spherical particles were observed when a Nile-red-encapsulated vesicular solution was examined under a florescence microscope (Figure 4c), thus confirming encapsulation.

Next, to examine the encapsulation of hydrophilic guests, a vesicular solution was mixed with the hydrophilic dye Calcein. Extensive dialysis was carried out to ensure the complete removal of any unencapsulated dye and then the emission spectrum of the solution was checked, which showed a distinct emission band at 510 nm, owing to encapsulated Calcein (Figure 5a). When the emission intensity of the vesicle-encapsulated dye was compared with that of the absorption-normalized aqueous solution of the free dye, self-quenching was observed in former case, which could be attributed to the confinement effect.[24] In this case, fluorescence microscopy images revealed green-light-emitting spherical particles (Figure 5b), as expected from the location of the emission band of Calcein. In the absence of any dye, the original vesicular aggregates appeared as weakly green-light-emitting particles (see the Supporting Information, Figure S5), which was in accordance with the emission

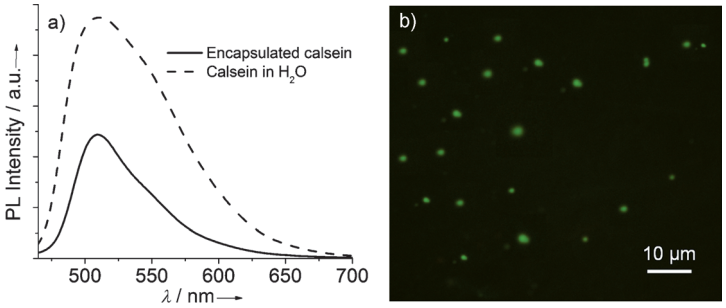

Figure 5. a) Absorbance-normalized emission spectra of Calcein ($\lambda_{ex}=$ 450 nm) that is encapsulated inside **NDI-1** vesicles (solid line) and in bulk (dotted line); b) fluorescence microscopy images of Calcein-encapsulated **NDI-1** vesicles.

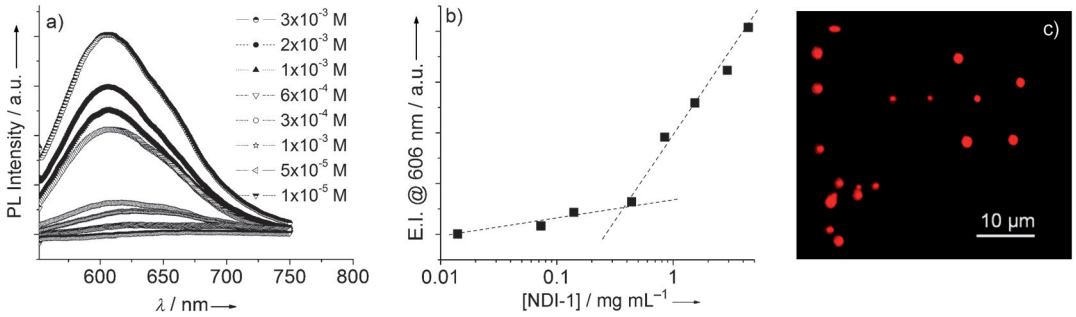

Figure 4. a) Emission spectra ($\lambda_{ex}=530$ nm) of Nile red that is encapsulated inside solutions of **NDI-1** vesicles of various concentrations. b) Variation in the emission intensity of Nile red at 606 nm as a function of the concentration **of NDI-1**. c) Fluorescence microscopy images of Nile-red-encapsulated **NDI-1** vesicles.

© 2012 Wiley-VCH Verlag GmbH & Co. KGaA, Weinheim

These are not the final page numbers!

spectra of **NDI-1** chromophores (see the Supporting Information, Figure S5) in the aggregated state.

Because the denaturing agent, such as urea, was shown to destroy the hydrogen-bonding interactions and, consequently, π-stacking, we examined the effect of this agent on the release of encapsulated guest molecules from the vesicle. The gradual addition of urea to a Nile-red-encapsulated (hydrophobic guest) vesicle solution resulted in the appearance of a new emission peak at $\lambda_{max}=656$ nm (Figure 6a), which was where the emission band appeared for Nile red in bulk water.[25] The emission intensity at 656 nm was plotted (Figure 6a, inset) as a function of urea, which revealed the complete release in the presence of 130 mg of urea. Furthermore, we probed the urea-mediated release of encapsulated Calcein, which is a water-soluble probe unlike Nile red. In this case, emission intensity at 515 nm was plotted versus time (Figure 6b) and showed that the release of Calcein could be completed in about 3 h from the dialysis bag.

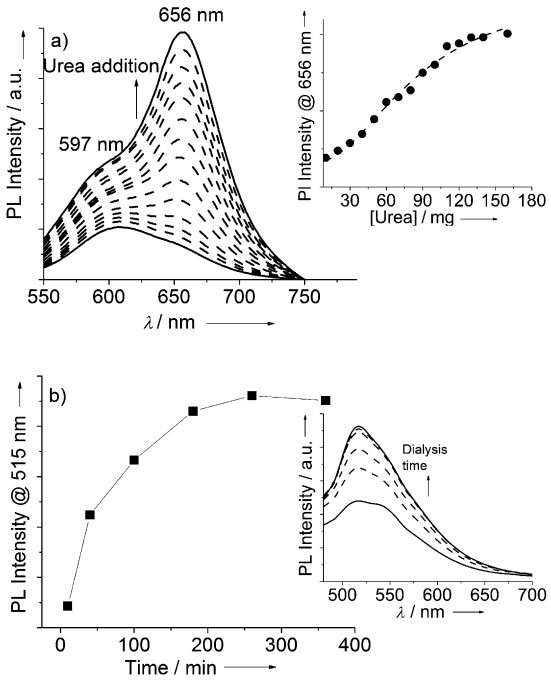

Figure 6. a) Release of vesicle-encapsulated Nile red with the addition of urea; inset: variation in emission intensity at 656 nm as a function of the concentration of urea. b) Time-dependent variation in the emission intensity of released Calcein at 515 nm with the addition of excess urea; inset: actual spectroscopic variation.

Pyrene intercalation and morphological transition (2D-to-1D): NDI is known to be a strong acceptor that forms stable CT complexes[26] with various donors, among which pyrene is the best candidate.[27] Thus, a curiosity-driven experiment was performed to examine the nature of the co-assembly in a mixed **NDI-1**/pyrene system (1:1). Because pyrene alone is not soluble in water, it was mixed with **NDI-1** in THF (1 mM each) when no visible color change was observed. However, upon evaporating the solvent, a deep-red, waxy material was obtained, thus indicating the formation of a CT complex. Dissolving this material in water (total chromophore concentration = 2 mM) afforded an optically clear red solution (Figure 7a). Remarkably, in the presence of **NDI-1**, hydrophobic pyrene molecules could be fully dissolved in water,[28] which suggests complete intercalation to induce an alternate donor–acceptor stacked assembly that is encased by peripheral oligo-oxyethylene chains. As expected from a cursory observation, a broad and intense CT-absorption band was noticed ($\lambda_{max}=532$ nm, Figure 7a). The association constant for the CT complex was estimated to be very high ($9.69\times10^3\,M^{-1}$) by monitoring the change in intensity of the CT band with concentration (see the Supporting Information, Figure S6) and fitting the data to a standard equation [Eq. (1), see the Experimental Section].[29] The energy-minimized structure of the alternate D–A stack was calculated, which predicted that the hydrazide functionalities could remain hydrogen-bonded among themselves, even after pyrene insertion (see the Supporting Information, Figure S7).

To gather experimental evidence, the FTIR spectrum of a solution of pyrene+**NDI-1** (1:1) was recorded, in which the ν(C=O) stretch of the hydrazide group appeared at 1645 cm^{-1} (see the Supporting Information, Figure S8), which closely matched that of **NDI-1** alone (1655 cm^{-1}). Furthermore, with the addition of urea, the CT-absorption band gradually decreased and completely diminished (Figure 7b) in the presence of 2.8 M denaturing agent, which strongly supported the involvement of hydrogen-bonding, even in the alternate D–A stacked assembly. Interestingly, upon prolonged standing (2–3 days), the red solution of pyrene+**NDI-1** became significantly more viscous and, at relatively high concentration (5 mM of each component), produced a transparent red gel[20] (Figure 8, inset) after 3 days. The critical gelation concentration and the gel-to-sol transition temperature were 0.3 wt.% and 53 °C, respectively. The morphology of the gel was examined

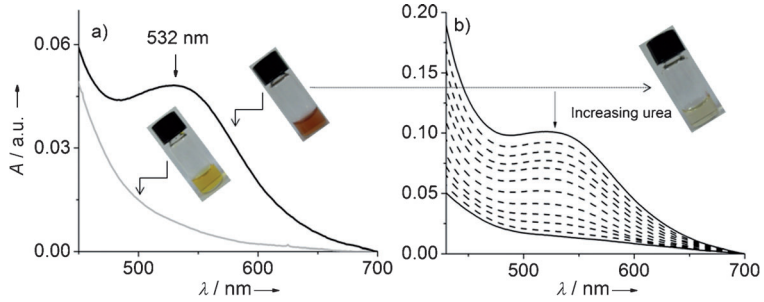

Figure 7. a) Selected region of the UV/Vis spectra of **NDI-1** (gray line) and **NDI-1**+pyrene (1:1, black line) and photographs of the two solutions ($c=5$ mM in each case). b) Effect of the addition of urea (up to 70 mg/0.5 mL 5.0 mM NDI solution) on the CT-absorption band; inset: disappearance of the red color of the solution in the presence of urea.

© 2012 Wiley-VCH Verlag GmbH & Co. KGaA, Weinheim

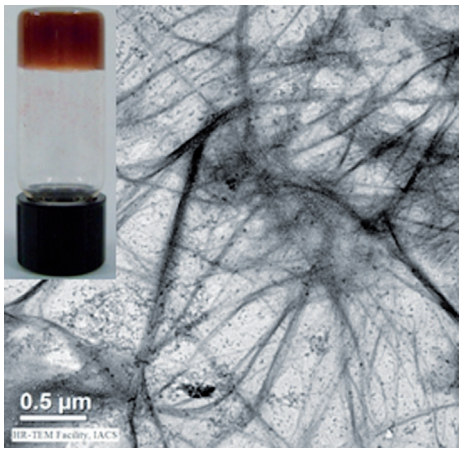

Figure 8. TEM images of the **NDI-1**+pyrene (1:1) gel; inset: photograph of the hydrogel (10 mM).

by TEM (Figure 8), which revealed the presence of micrometer-long 1D fibers, in sharp contrast to the spherical vesicular assemblies of **NDI-1** (Figure 3b). Notably, no such increase in viscosity or gelation was noticed for **NDI-1** alone, even at a concentration of 20 mM, which clearly suggested that the morphology transition (2D vesicle to 1D fiber) is directly related to pyrene intercalation. Furthermore, variable-temperature UV/Vis studies showed that the CT band disappeared above 50 °C, which is close to the T_g, thus further supporting that the gelation is directly related to CT complexation. Moreover, at 50 °C, the baseline intensity in the absorption spectra increased, thereby indicating the macroscopic precipitation of the pyrene guests owing to disassembly of the CT complex.

To investigate the mechanism of this morphological transition, AFM images of the mixed solution were recorded after different time intervals (Scheme 2). A freshly prepared sample showed the presence of individual spherical aggregates (Scheme 2, top-left image) with heights and diameters in the range (3.1 ± 0.1) nm and 80–100 nm, respectively. The diameter of the particles almost doubled after 24 h with the occasional signature of an interparticle assembly (Scheme 2, top-middle). After 48 h, individual spherical particles coagulated together (Scheme 2, top-right image), which eventually resulted in the generation of 1D fibers after 72 h (Scheme 2, bottom-left image). Based on these experimental results, we proposed that, owing to pyrene intercalation, the radius of curvature of the membrane increases[8f] to accommodate the additional strain that was induced by the intercalator. This induced-swelling of the vesicular particles eventually leads to intervesicle aggregation and, finally, to rupturing of the membrane (to release the strain) to produce 1D fibers. In addition to the AFM data, this model was also supported by DLS studies (see the Supporting Information, Figure S9), which revealed a gradual increase in the hydrodynamic radius of the particles from about 40 nm to about 100 nm over first 3 days, followed by an abrupt increase to the range of microns, thus revealing the generation of elongated 1D fibers with a much-larger hydrodynamic radius.

Intercalation-mediated functionalization of vesicles: The intercalation of pyrene prompted us to explore the possible in situ non-covalent functionalization of the vesicular membrane by functionalized pyrene. Thus, an aqueous solution of the sodium salt of pyrene butyric acid (which is soluble in water, unlike pyrene) was mixed with **NDI-1** (1:1) and spontaneously produced an intense green-colored solution (Figure 9a, inset). Accordingly, a new absorption band appeared with $\lambda_{max} = 575$ nm, thus suggesting CT complexation.

Green coloration of the solution, in contrast to the commonly seen red color for the pyrene/NDI CT complex, can be attributed to the modified HOMO energy level of substituted pyrene compared to the unsubstituted chromo-

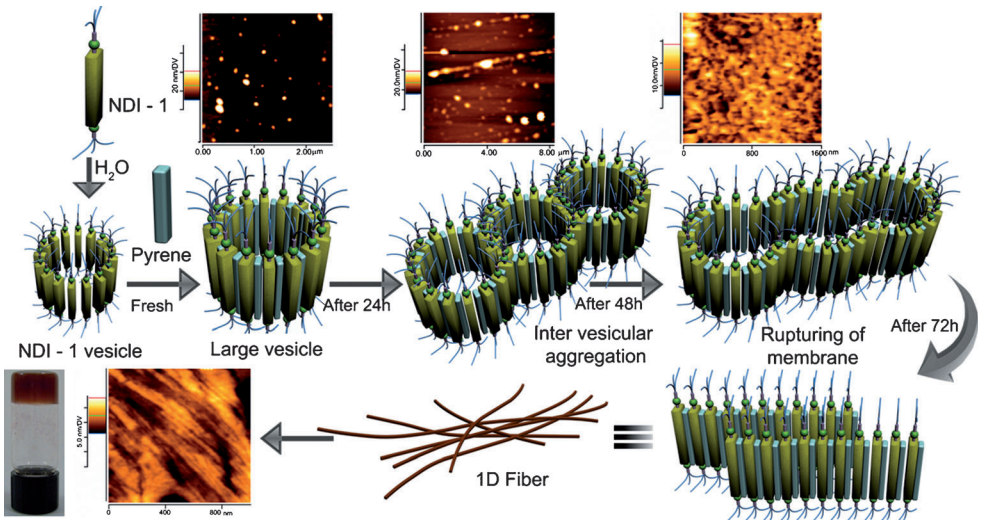

Scheme 2. Proposed model for the guest-induced stepwise morphological transition from 2D vesicles to 1D fibers for **NDI-1**, thereby leading to gelation (gel image is shown in the bottom-left corner).

© 2012 Wiley-VCH Verlag GmbH & Co. KGaA, Weinheim

These are not the final page numbers!

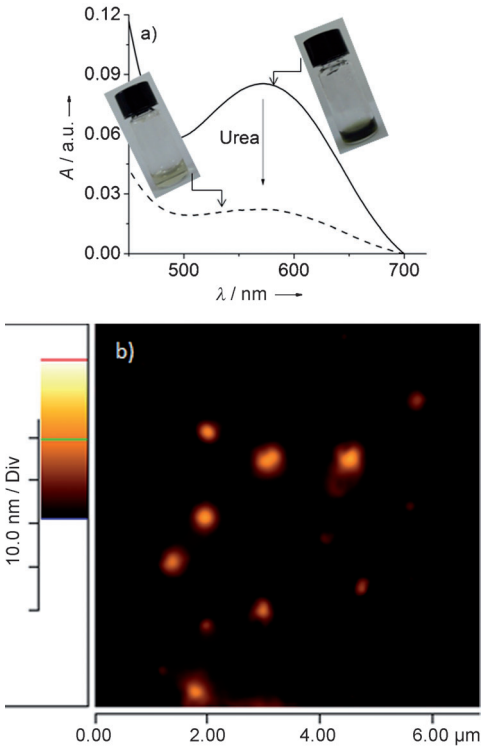

Figure 9. a) Selected region of UV/Vis spectra of **NDI-1**+pyrene butyrate (1:1) before (black line) and after (red line) the addition of urea (120 mg); total concentration of the chromophore = 5 mM, solution volume = 0.2 mL, path length of the cuvette = 1 mm. b) AFM height images of an aqueous solution of **NDI-1**+pyrene butyrate (1:1, $c = 1$ mM).

phore.[30] As above, in this case, the CT band also disappeared in the presence of excess urea (Figure 9a) and, consequently, the green solution became almost colorless (Figure 9a, inset), thus confirming the existence of hydrogen-bonding. In this case, the association constant of the CT complex was estimated to be $1.65 \times 10^3\,M^{-1}$ by using a similar procedure (see the Supporting Information, Figure S10). AFM images (Figure 9b) showed spherical particles with an average height and width of (10 ± 1) and (200 ± 20) nm, respectively, thereby confirming that the vesicular morphology remained intact, even in the presence of the carboxylate-functionalized intercalator. However, as a result of intercalation, the size of the vesicles increased almost two fold, possibly owing to a release of the strain that was imposed by intercalation. This result was well-supported by the DLS data (see the Supporting Information, Figure S11), in which the average size of the functionalized vesicular particles was estimated to be 100 nm, which is significantly larger than that of **NDI-1** alone. Surprisingly, unlike previous example of the intercalation of unsubstituted pyrene, in this case, no increase in viscosity was observed with time and, even after several days, the solution did not transformed into a gel, even when the concentration was increased to 20 mM. This result is attributed to electrostatic repulsion between the carboxylate-functionalized vesicles, which prohibited interparticle aggregation, a key step for vesicle-to-fiber morphological transition (Scheme 2).

In an attempt to tune the extent of surface functionalization, the amount of intercalator was varied, which produced solutions with different CT-band intensities (Figure 10a). The absorbance at 575 nm was plotted against the concentration of the intercalator and showed an ideal linear behavior (Figure 10, inset), thereby suggesting tunable functionalization. To get a more-direct confirmation of this surface functionalization, zeta-potential measurements were carried out, which revealed negative values (Figure 10) for all of the samples, thus suggesting the presence of negatively charged particles, as expected for carboxylate-functionalized vesicles. More importantly, the potential could be tuned by changing the amount of intercalator, which suggested that this approach could produce the tunable in situ surface functionalization of a vesicular membrane. However, the variation in zeta potential was not as regular as the intensity of the CT band. This result is because, with an increasing amount of intercalator, the size of the particles increased from about 40 nm to 100 nm (see the Supporting Information, Figure S11), but not in a perfect linear fashion. Because the zeta potential is a measure of the charge/size of a given particle, the value does not solely depend on the charge density.

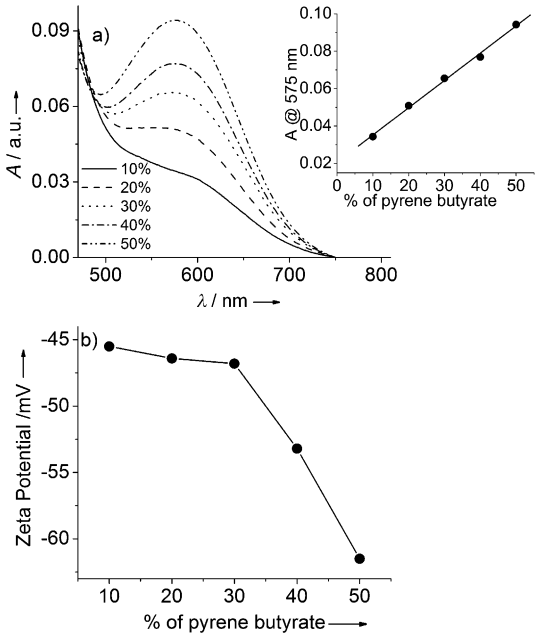

Figure 10. a) UV/Vis spectra of **NDI-1**+pyrene butyrate (various ratios, total concentration = 2 mM); inset: intensity of the CT band at 575 nm as a function of the concentration of pyrene butyrate. b) Variation of the zeta potential of solutions of **NDI-1**+pyrene butyrate (total concentration = 2 mM) with various concentrations of intercalator.

© 2012 Wiley-VCH Verlag GmbH & Co. KGaA, Weinheim

Conclusion

In summary, we have reported the vesicular assembly of a bis-hydrazide-functionalized NDI-based bolaamphiphile in aqueous medium by using the synergistic effect of hydrogen-bonding and π-stacking interactions. Control experiments clearly showed the necessity of proper placement of the hydrazide functionality to ensure shielding from the bulk water so that they could remain engaged amongst themselves in intermolecular hydrogen-bonding. Furthermore, the electron-deficient NDI chromophores in the vesicular membrane quite-remarkably provided space for the intercalation of completely water-insoluble electron-rich pyrene guest molecules in a stoichiometric ratio to gain additional stabilization through CT interactions without disrupting the hydrogen-bonding framework. Interestingly, such intercalation-induced 2D-to-1D vesicle-to-fiber morphological transitions through intervesicular fusion eventually resulted in gelation at higher concentrations. This process could be further extended to achieve a tunable, in situ, non-covalent functionalization of the membrane by using a water-soluble-functionalized intercalator, such as pyrene butyrate. These results could inspire the exploration of various other directional non-covalent interactions to enrich the field of self-assembly of amphiphilic molecules and macromolecules to generate complex self-assembled functional materials. In particular, it will be interesting to examine such NDI-based vesicles as model systems to understand the fusion of cell membranes and also for selective ion-transport.[17] Intercalation-based non-covalent surface-functionalization approaches may also find great relevance in areas such as targeted delivery and sensing; currently, such efforts are underway in our laboratory.

Experimental Section

UV/Vis spectroscopy: In a typical UV/Vis experiment, a stock solution of **NDI-1** (20 mM) was made in THF, from which an aliquot (0.1 mL) was transferred into a glass vial and the solvent was evaporated to produce a thin film. To this film was added a measured amount of THF/water to adjust the desired final concentration (1 mM) of the solution and the vial was shaken vigorously to produce an optically clear solution. The solution was allowed to equilibrate at RT for 2 h before spectroscopic measurements were recorded.

Atomic force microscopy (AFM): An aqueous solution of **NDI-1** (20 μL, 1 mM) was placed on a silicon wafer and allowed to dry overnight in air before the images were taken. In the case of the hydrogel, the gel (0.1 mL, 5 mM) was diluted with water (0.1 mL) and the samples were prepared by following a similar procedure to that described above.

Transmission electron microscopy (TEM): A solution of the sample in water (20 μL, 1 mM) was placed on a TEM grid (300 mesh carbon-coated Cu grid). The samples were allowed to dry under vacuum for a few hours before the measurements were recorded.

FTIR spectroscopy: A solution of the sample in either THF or water (50 μL, 2 mM) was placed in the spectroscopic cell, which was sandwiched between two CaF_2 windows, and the spectra of the solutions were recorded.

X-ray diffraction: XRD data were recorded on a Seifert XRD3000P diffractometer with Cu Kα radiation ($\alpha = 0.15406$ nm) and a voltage and a current of 40 kV and 30 mA, respectively. In a typical XRD experiment, a solution of **NDI-1** in water (1 mM) was repeatedly drop-cast onto a glass slide to make a thick film. The film was then dried under a high vacuum and the data were recorded from 1–30° with a sampling interval of 0.02°/step.

Fluorescence microscopy: A solution of **NDI-1** (40 μL) and various dye-encapsulated solutions were placed between two clean glass slips and images were taken on a fluorescence microscope (OLIMPUS BX-61) at ×40 magnification.

Determination of the critical aggregation concentration (CAC): The CAC of **NDI-1** was determined by using two independent methods: In the first method, a stock solution of **NDI-1** in water (10 mM) was prepared and from this a series of solutions of various concentrations were produced (1–0.05 mM) that were equilibrated for 1 h at RT before UV/Vis spectroscopic analysis. Then, the absorbance of **NDI-1** at 380 nm was plotted against concentration and the CAC value was estimated from the inflection point. In the second method (fluorescence method by Nile-red encapsulation), a measured amount of a solution of Nile red in THF (100 μL, 0.1 mM) was placed in various screw-capped vials and the solvent was evaporated. Solutions of various concentrations of **NDI-1** were added to vials that contained Nile red and the mixture was sonicated and allowed to stand for 2 h before fluorescence spectroscopic analysis ($\lambda_{ex} =$ 530 nm). The final concentration of Nile red was 10^{-5} M. The emission intensity of the encapsulated Nile red at 606 nm was plotted versus the concentration of **NDI-1** and the inflection point of such a plot was taken as the CAC of **NDI-1**.

Dynamic light scattering (DLS): DLS experiments were carried out on a Malvern instrument. A solution of (2 mL, 1 mM) the sample was prepared and equilibrated at RT for 2 h before the DLS analysis.

Calcein encapsulation: An aqueous solution of Calcein (0.2 mL, 10^{-3} M) was mixed with a solution of **NDI-1** in water (1.8 mL, final concentration of **NDI-1** = 1 mM) and the mixture was sonicated for 15 min and then stirred overnight at RT. The mixture was further dialyzed against water by using 3000 Da MWCO membrane for 48 h (outside water was replaced with fresh water every 2 h) to remove any unencapsulated dye. Then, the fluorescence spectra of the dialyzed solution was recorded and compared with an absorption-normalized aqueous solution of the free dye.

Calcein-release experiment: A solution of **NDI-1** vesicles (2 mL, 1 mM) was treated with Calcein and extensive dialysis was performed to remove any unencapsulated dye. When no more dye was coming out (confirmed by the lack of an emission band from the water outside the dialysis bag), excess urea (about 200 mg) was added to the solution inside the dialysis bag and the bag was dipped into a container of fresh water (20 mL), from which an aliquot (0.5 mL) was taken and emission spectra were recorded at different time intervals.

Gelation test and the determination of T_{gel}: Solutions of **NDI-1** and pyrene (0.2 mL, 10 mM each) in THF were mixed together and the solvent was evaporated to produce a deep-red-colored thin film; 0.4 mL water was added and the mixture was sonicated for 3 min to produce an optically clear red solution. The solution was allowed to stand for 3 days at RT, after which time gelation was noted by the "stable to inversion of a vial" method. The T_{gel} value was determined by using the "dropping-ball" method: In a typical experiment, a glass ball (weight: 85.0 mg) was slowly placed on top of the gel (10 mM) in a screw-capped vial and then the vial was placed in a water bath. The temperature of the water bath was gradually increased and the temperature at which the ball touched the bottom of the vial was taken as T_{gel} (the gel-to-sol transition temperature).

Determination of the association constant (K_a) for the CT complex: A deep-red-colored solution of **NDI-1**+pyrene (10 mM, 1:1) was gradually diluted with water and spectra were recorded at each concentration. The intensity of the CT-absorption band at 529 nm was monitored at each concentration and, from this data, the association constant (K_a) was determined according to Equation (1), in which c, A, ε, and l are the concentration, absorbance, extinction coefficient, and optical path length of the cuvette, respectively ($l = 0.1$ cm). To obtain the association constant,

© 2012 Wiley-VCH Verlag GmbH & Co. KGaA, Weinheim

These are not the final page numbers!

c/A was plotted against $1/A^{1/2}$; K_a was calculated from the slope of the plot.

$$\frac{c}{A} = \frac{1}{\sqrt{K_a \varepsilon l}} \frac{1}{\sqrt{A}} + \frac{1}{\varepsilon l} \quad (1)$$

Zeta potential: Measurements were carried out on a Malvern instrument. Stock solutions of pyrene butyrate (10 mM) and **NDI-1** (10 mM) were mixed in various ratios and diluted with water to make final total chromophoric concentration of 1 mM. All of the solutions were equilibrated at RT for 1 h before the experiments were performed.

Acknowledgements

S.G. thanks the Department of Science and Technology (DST), New Delhi, India, (Project No. SR/FT/CS-039/2008) for financial support. M.R.M. thank the IACS for a research fellowship. We thank Ms. Ujwala Das for performing the DLS measurements and Mr. Gopal Krishna Manna for helping us to prepare Scheme 1 and Scheme 2.

[1] D. F. Evans, H, Wennerstrom, *The Colloidal Domain* 2nd ed.; Wiley-VCH: New York, **1999**.

[2] a) R. K. O'Reilly, C. J. Hawker, K. L. Wooley, *Chem. Soc. Rev.* **2006**, *35*, 1068; b) A. Blanazs, S. P. Armes, A. J. Ryan, *Macromol. Rapid Commun.* **2009**, *30*, 267; c) T. S. Kale, A. Klaikherd, B. Popere, S. Thayumanavan, *Langmuir* **2009**, *25*, 9660.

[3] a) J-M. Lehn, *Science* **2002**, *295*, 2400; b) G. M. Whitesides, J. P. Mathias, C. T. Seto, *Science* **1991**, *254*, 1312; c) L. Brunsveld, B. J. B. Folmer, E. W. Meiher, R. P. Sijbesma, *Chem. Rev.* **2001**, *101*, 4071; d) Z. Chen, A. Lohr, C. R. Saha-Möller, F. Würthner, *Chem. Soc. Rev.* **2009**, *38*, 564.

[4] a) H. Shao, J. Seifert, N. C. Romano, M. Gao, J. J. Helmus, C. P. Jaroniec, D. A. Modarelli, J. R. Parquette, *Angew. Chem.* **2010**, *122*, 7762; *Angew. Chem. Int. Ed.* **2010**, *49*, 7598; b) M. Kumar, S. J. George, *Nanoscale* **2011**, *3*, 2130; c) G. Fernández, F. García, L. Sánchez, *Chem. Commun.* **2008**, 6567; d) X. Zhang, S. Rehm, M. M. Safont-Sempere, F. Würthner, *Nat. Chem.* **2009**, *1*, 623; e) X. Zhang, Z. Chen, F. Würthner, *J. Am. Chem. Soc.* **2007**, *129*, 4886; f) S. H. Seo, J. Y. Chang, G. N. Tew, *Angew. Chem.* **2006**, *118*, 7688; *Angew. Chem. Int. Ed.* **2006**, *45*, 7526; g) K. S. Moon, H.-J. Kim, E. Lee, M. Lee, *Angew. Chem.* **2007**, *119*, 6931; *Angew. Chem. Int. Ed.* **2007**, *46*, 6807; h) B. Schade, K. Ludwig, C. Böttcher, U. Hartnagel, A. Hirsch, *Angew. Chem.* **2007**, *119*, 4472; *Angew. Chem. Int. Ed.* **2007**, *46*, 4393; i) D. A. Stone, L. Hsu, S. I. Stupp, *Soft Matter* **2009**, *5*, 1990; j) J. F. Hulvat, M. Sofos, K. Tajima, S. I. Stupp, *J. Am. Chem. Soc.* **2005**, *127*, 366; k) A. F. M. Kilbinger, A. P. H. J. Schenning, F. Goldoni, W. J. Feast, E. W. Meijer, *J. Am. Chem. Soc.* **2000**, *122*, 1820.

[5] a) K. Liu, C. Wang, Z. Li, X. Zhan, *Angew. Chem.* **2011**, *123*, 5054; *Angew. Chem. Int. Ed.* **2011**, *50*, 4952; b) X. Zhang, C. Wang, *Chem. Soc. Rev.* **2011**, *40*, 94.

[6] a) Y. Hong, J. W. Y. Lam, B. Z. Tang, *Chem. Soc. Rev.* **2011**, *40*, 5361; b) F. J. M. Hoeben, P. Jonkheijm, E. W. Meijer, A. P. H. J. Schenning, *Chem. Rev.* **2005**, *105*, 1491; c) A. Ajayaghosh, V. K. Praveen, C. Vijayakumar, *Chem. Soc. Rev.* **2008**, *37*, 109.

[7] a) For a recent review on hydrogen-bonding-mediated supramolecular assembly, see: D. González-Rodríguez, A. P. H. J. Schenning, *Chem. Mater.* **2011**, *23*, 310; b) G. R. Desiraju, *Angew. Chem.* **1995**, *107*, 2541; *Angew. Chem. Int. Ed. Engl.* **1995**, *34*, 2311.

[8] a) N. Kimizuka, T. Kawasaki, T. Kunitake, *J. Am. Chem. Soc.* **1993**, *115*, 4387; b) T. Kawasaki, M. Tokuhiro, N. Kimizuka, T. Kunitake, *J. Am. Chem. Soc.* **2001**, *123*, 6792; c) P. Besenius, G. Portale, P. H. H. Bomans, H. M. Janssen, A. R. A. Palmans, E. W. Meijer, *Proc. Natl. Acad. Sci. USA* **2010**, *107*, 17888; d) T. M. Hermans, M. A. C. Broeren, N. Gomopoulos, A. F. Smeijers, B. Mezari, E. N. M. Van Leeuwen, M. R. J. Vos, P. C. M. M. Magusin, P. A. Hilbers, M. H. P. Van Genderen, N. A. J. M. Sommerdijk, G. Fytas, E. W. Meijer, *J. Am. Chem. Soc.* **2007**, *129*, 15631; e) A. Pal, P. Besenius, R. P. Sijbesma, *J. Am. Chem. Soc.* **2011**, *133*, 12987; f) Z. Yang, X. Wang, Y. Yang, Y. Liao, Y. Wei, X. Xie, *Langmuir* **2010**, *26*, 9386.

[9] a) S. V. Bhosale, C. H. Jani, S. Langford, *Chem. Soc. Rev.* **2008**, *37*, 331; b) N. Sakai, J. Mareda, E. Vauthey, S. Matile, *Chem. Commun.* **2010**, *46*, 4225.

[10] a) B. A. Jones, A. Facchetti, M. R. Wasielewski, T. J. Marks, *J. Am. Chem. Soc.* **2007**, *129*, 15259; b) B. J. H. Oh, S. L. Suraru, W. Y. Lee, M. Könemann, H. W. Höffken, C. Röger, R. Schmidt, Y. Chung, W. C. Chen, F. Würthner, Z. Bao, *Adv. Funct. Mater.* **2010**, *20*, 2148.

[11] P. Mukhopadhyay, Y. Iwashita, M. Shirakawa, S.-i. Kawano, N. Fujita, S. Shinkai, *Angew. Chem.* **2006**, *118*, 1622; *Angew. Chem. Int. Ed.* **2006**, *45*, 1592.

[12] a) H. Y. Au-Yeung, G. D. Pantos, J. K. M. Sanders, *Angew. Chem.* **2010**, *122*, 5459; *Angew. Chem. Int. Ed.* **2010**, *49*, 5331; b) H. Y. Au-Yeung, G. D. Pantos, J. K. M. Sanders, *Proc. Natl. Acad. Sci. USA* **2009**, *106*, 10466; c) H. Y. Au-Yeung, G. D. Pantos, J. K. M. Sanders, *J. Am. Chem. Soc.* **2009**, *131*, 16030.

[13] a) S. A. Vignon, T. Jarrosson, T. Iijima, H.-R. Tseng, J. K. M. Sanders, J. F. Stoddart, *J. Am. Chem. Soc.* **2004**, *126*, 9884; b) T. Iijima, S. A. Vignon, H. R. Tseng, T. Jarrosson, J. K. M. Sanders, F. Marchioni, M. Venturi, E. Apostoli, E. Balzani, J. F. Stoddart, *Chem. Eur. J.* **2004**, *10*, 6375.

[14] a) R. S. Lokey, B. L. Iverson, *Nature* **1995**, *375*, 303; b) J. J. Reczek, K. R. Villazor, V. Lynch, T. M. Swager, B. L. Iverson, *J. Am. Chem. Soc.* **2006**, *128*, 7995; c) A. J. Zych, B. L. Iverson, *J. Am. Chem. Soc.* **2000**, *122*, 8898; d) M. S. Cubberley, B. L. Iverson, *J. Am. Chem. Soc.* **2001**, *123*, 7560; e) G. J. Gabriel, B. L. Iverson, *J. Am. Chem. Soc.* **2002**, *124*, 15174; f) R. W. Sinkeldam, F. J. M. Hoeben, M. J. Pouderoijen, I. D. Cat, J. Z. S. Furukawa, S. D. Feyter, J. A. J. M. Vekemans, E. W. Meijer, *J. Am. Chem. Soc.* **2006**, *128*, 16113; g) S. De, S. Ramakrishnan, *Chem. Asian J.* **2011**, *6*, 149.

[15] a) H. Shao, J. R. Parquette, *Chem. Commun.* **2010**, *46*, 4285; b) H. Shao, T. Nguyen, N. C. Romano, D. A. Modarelli, J. R. Parquette, *J. Am. Chem. Soc.* **2009**, *131*, 16374.

[16] a) S. Bhosale, A. L. Sisson, P. Talukdar, A. Fürstenberg, N. Banerji, E. Vauthey, G. Bollot, J. Mareda, C. Röger, F. Würthner, N. Sakai, S. Matile, *Science* **2006**, *313*, 84; b) R. Bhosale, J. Míšek, N. Sakai, S. Matile, *Chem. Soc. Rev.* **2010**, *39*, 138; c) N. Sakai, A. L. Sisson, T. Bürgi, S. Matile, *J. Am. Chem. Soc.* **2007**, *129*, 15758.

[17] a) R. E. Dawson, A. Hennig, D. P. Weimann, D. Emery, V. Ravikumar, J. Montenegro, T. Takeuchi, S. Gabutti, M. Mayor, J. Mareda, C. A. Schalley, S. Matile, *Nat. Chem.* **2010**, *2*, 533; b) P. Talukdar, G. Bollot, J. Mareda, N. Sakai, S. Matile, *J. Am. Chem. Soc.* **2005**, *127*, 6528; c) J. Mareda, S. Matile, *Chem. Eur. J.* **2009**, *15*, 28; d) A. L. Sisson, M. R. Shah, S. Bhosale, S. Matile, *Chem. Soc. Rev.* **2006**, *35*, 1269.

[18] a) M. R. Molla, A. Das, S. Ghosh, *Chem. Eur. J.* **2010**, *16*, 10084; b) A. Das, S. Ghosh, *Chem. Commun.* **2011**, *47*, 8922.

[19] a) M. R. Molla, S. Ghosh, *Chem. Mater.* **2011**, *23*, 95; b) A. Das, M. R. Molla, S. Ghosh, *J. Chem. Sci.* **2011**, *123*, 963; c) A. Das, M. R. Molla, B. Maity, D. Koley, S. Ghosh, *Chem. Eur. J.*, DOI: 10.1002/chem.201201140.

[20] For CT-interaction-mediated gelation, see: a) K. V. Rao, K. Jayaramulu, T. K. Maji, S. J. George, *Angew. Chem.* **2010**, *122*, 4314; *Angew. Chem. Int. Ed.* **2010**, *49*, 4218; b) R. K. Das, S. Banerjee, G. Raffy, A. D. Guerzo, J.-P. Desvergne, U. Maitra, *J. Mater. Chem.* **2010**, *20*, 7227.

[21] For CT-interaction-mediated morphological transitions in supramolecular amphiphilic systems, see: C. Wang, S. Yin, S. Chen, H. Xu, Z. Wang, X. Zhang, *Angew. Chem.* **2008**, *120*, 9189; *Angew. Chem. Int. Ed.* **2008**, *47*, 9049.

[22] W. Wang, L.-S. Li, G. Helms, H.-H. Zhou, A. D. Q. Li, *J. Am. Chem. Soc.* **2003**, *125*, 1120.

[23] a) D. R. Canchi, D. Paschek, A. E. García, *J. Am. Chem. Soc.* **2010**, *132*, 2338; b) A. Das, C. Mukhopadhyay, *J. Phys. Chem. B* **2009**, *113*, 12816; c) E. P. O'Brien, R. I. Dima, B. Brooks, D. Thirumalai, *J.*

 © 2012 Wiley-VCH Verlag GmbH & Co. KGaA, Weinheim

Am. Chem. Soc. **2007**, *129*, 7346; d) A. Wallqvist, D. G. Covell, *J. Am. Chem. Soc.* **1998**, *120*, 427.

[24] E. N. Savariar, S. V. Aathimanikandan, S. Thayumanavan, *J. Am. Chem. Soc.* **2006**, *128*, 16224.

[25] Unexpectedly, the emission intensity of hydrophobic Nile red in aqueous medium increased as a function of release. To explain this apparent anomaly, we examined the emission spectra of Nile red (dispersed in water) and found that, with the addition of urea, the intensity increased (see the Supporting Information, Figure S12). Thus, in the presence of urea, whilst the observed red shift in the λ_{em} value is attributed to release, the unexpected increase in emission intensity is attributed to non-specific interactions of the dye with urea. See: P. Hazra, D. Chakrabarty, A. Chakraborty, N. Sarkar, *Chem. Phys. Lett.* **2004**, *388*, 150.

[26] R. Forster in *Organic Charge-Transfer Complex*, Academic Press, London, **1969**.

[27] N. S. S. Kumar, M. D. Gujrati, J. N. Wilson, *Chem. Commun.* **2010**, *46*, 5464.

[28] a) M. A. C. Broeren, J. G. Linhardt, H. Malda, B. F. M. de Waal, R. M. Versteegen, J. T. Meijer, D. W. P. M. Löwik, J. C. M. v. Hest, M. H. P. v Xendern, E. W. Meijer, *J. Polym. Sci. Part A* **2005**, *43*, 6431; b) D. Chun, F. Wudl, A. Nelson, *Macromolecules* **2007**, *40*, 1782.

[29] a) M. B. Nielsen, J. O. Jeppesen, J. Lau, C. Lomholt, D. Damgaard, J. P. Jacobsen, J. Becher, J. F. Stoddart, *J. Org. Chem.* **2001**, *66*, 3559; b) S. De, D. Koley, S. Ramakrishnan, *Macromolecules* **2010**, *43*, 3183.

[30] For a literature report that is related to the appearance of a CT band at relatively longer wavelength for a [substituted pyrene+NDI] complex, see: H. M. Colquhoun, Z. Zhu, D. J. Williams, *Org. Lett.* **2003**, *5*, 4353.

Received: April 17, 2012
Published online: ■■ ▮▮, 0000

 © 2012 Wiley-VCH Verlag GmbH & Co. KGaA, Weinheim

These are not the final page numbers!

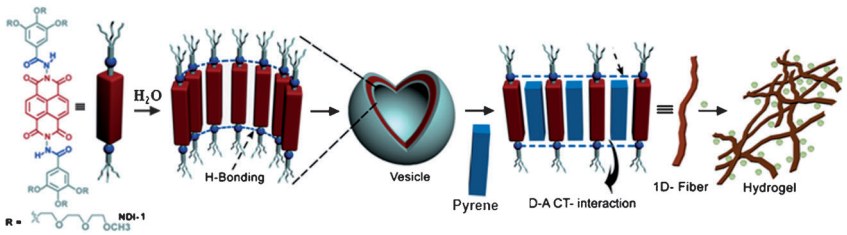

Fruit and fibers: Vesicular assembly of a NDI-based bolaamphiphile was achieved by using π-stacking and hydrogen-bonding in water. Pyrene intercalation resulted in a transition from 2D vesicles into 1D fibers and gelation at higher concentrations.

Hydrogen Bonds

*M. R. Molla, S. Ghosh** ..... ▮▮▮▮–▮▮▮▮

Hydrogen-Bonding-Mediated Vesicular Assembly of Functionalized Naphthalene–Diimide-Based Bolaamphiphile and Guest-Induced Gelation in Water

© 2012 Wiley-VCH Verlag GmbH & Co. KGaA, Weinheim